Control and implementation of a Permanent Magnet Synchronous Motor in a CowBrush unit

E. Olesen, R. Starup-Hansen, K. Labata

Department of Materials and Production, Aalborg University
Fibigerstraede 16, DK-9220 Aalborg East, Denmark
Email: eolese15, rstaru18, klabat18@student.aau.dk,
Web page: http://www.mechman.mp.aau.dk/

Abstract
In this project a study of a previous model of a Cowbrush has been studied in order to optimize its mechanical design and upgrade it so it can be run by a Permanent Magnet Synchronous Motor instead of the previous single phase AC motor. Besides this, the drive train has also been changed from a worm gear to a 4.5:1 belt drive. This modifications entail changes in both the electrical part of the system, for which a new inverter had to be designed, and control part, which uses a Digital Signal Processor and Field Oriented Control to control the electromechanical system.

Keywords: Cowbrush, PCB, PMSM, Field Oriented Control, Inverter design

1. Introduction

A recent law in Denmark [1] requires dairy cattle farms to provide at least one automatic Cowbrush unit per 50 cows. The supposed reason for this change is stated in the article from [2], where a scientific study has shown a 30% reduction in mastitis, which is an udder infection. Besides this, it also shows an attractive increase in the milk production, where the best study shows an increase of one liter of milk per cow per day. On the other hand one of the disadvantages of the Cowbrushes is the risk for the cow to get its tail entangled in the brush and torn off.

A Danish company called GEA Farm Technologies Mullerup A/S, provides two different Brush units, namely an E and M-brush. The drive train of GEA's Brushes has been studied in an earlier semester project at AAU, where it was found that the drive train was inefficient (21%) due to a single phase induction machine coupled with a wormgear [3]. The concept study was done for a physical E-brush, that was given to AAU, and can be seen at Fig.1.

Therefore GEA is interested in a new updated Cowbrush version, where the drive train is replaced with a more efficient concept. Besides the efficiency, a desired control of the brush also needs to be taken into account. This has lead to the following wishes and requirements from GEA.

Fig. 1 Example of an E-brush already implemented in a farm.

Requirements

- A simple transmission solution with a motor and gear integrated in one unit.
- An improved efficiency.
- Voltage- and frequency-independent solution with a grid connection of 90-265V AC and 50/60Hz.
- Universal application.

Wishes

- A transmission system which is not self locking, which allows the cows to disentangle their tails so they do not get torn off.
- An electrical control that activates the brush when

the housing is rotated more than 5°, and maintains a constant brush speed of around 35Rpm.
- A control structure that changes the direction of rotation at a desired sequence to get an evenly wear of the brush bristles.
- An economically attractive solution that matches or reduces the original transmission costs.

The article will, in section 2, describe how a mechanical drive train is developed whose structure is built such that it is universal and can be integrated into different units.

In section 3 it will describe how a electrical circuit is designed to control a Permanent Magnet Synchronous Motor that drives the mechanical transmission.

In section 4 it will describe how the electromechanical power transmission is modelled and how the system parameters is identified.

In section 5 it will describe how the electromechanical system is controlled, by the use of Field Orientated Control.

Finally in section 6 a conclusion summarizes the achieved results from the work.

2. Mechanical Concept Design

The concept design is based on a simple functional analysis, which is limited to concern a chain/belt transmission because of their high efficiency performances [4].

2.1 Transmission principle

In the analysis three different concepts are compared, which are shown at Fig.2.

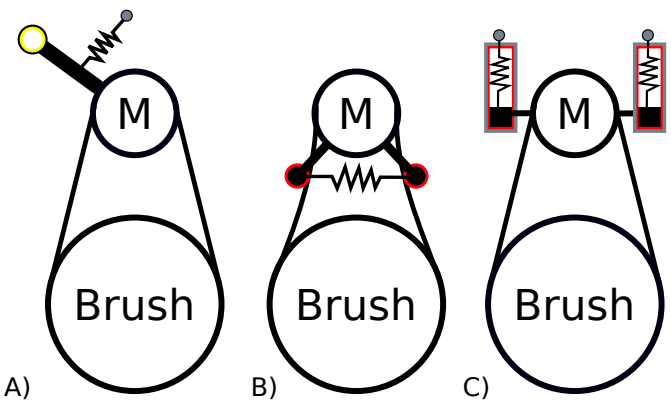

Fig. 2 Transmission principles A, B and C.

On the Fig.2 the M denotes the motor and pulley which are integrated in one unit. $Brush$ denotes the pulley that is attached to the brush shaft and thereby rotates the brush when the motor rotates.

Of the three principles, the A principle is chosen because of the simplicity and number of elements. Here, the tension of the belt/chain can be done with a linear or torsional spring.

2.2 Selection of the belt

It is chosen to use a belt drive instead of a chain drive for the following reasons: The belt drive is easier to maintain, does not require the same safety attention, does not need lubricants and can be adjusted to slip if overload is applied to protect the PMSM.

A disadvantage of the belt drive compared to the chain is a better life time and more compact design.

There exist a variety of standard belts which could be utilized for the transmission. Here a polyvee belt is chosen, because it has one of the smallest possible pulley dimensions together with the flat belt and timing belt. Besides this, it has a higher capacity than a flat belt and the pulley is easier to manufacture than a gear for a timing belt.

2.3 Structural Construction

CAD drawings are developed for the transmission principle, and implemented in the existing housing, which is shown in Fig. 3.

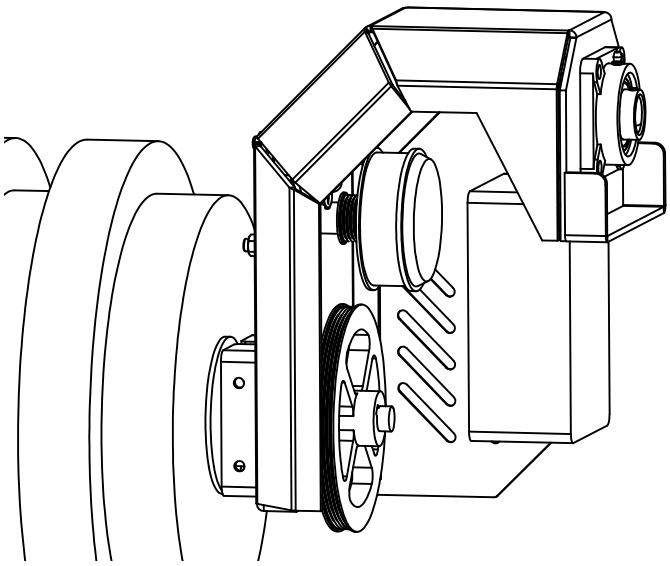

Fig. 3 A close-up of the Cow-housing CAD-drawing with the mechanical concept implemented

The principle is constructed with a support plate consisting of a shaft for the motor arm and a tension

feature where the linear spring can be attached and elongated to a desired tension of the belt.

The motor arm is a simple profile with two tubes in each end which can be mounted on the shaft from the support plate and attached to the PMSM shaft.

Finally, a brush and motor pulley are constructed, where the motor pulley is screwed onto the rotor of the PMSM, which is possible since the motor type is an outrunner with a stationary shaft in the middle.

The constructed transmission has a gearing ratio of 4.5.

3. Printed Circuit Board Design

The electrical circuit to supply and control the PMSM is designed based on a general inverter, which through inversion transforms a DC voltage into three sinusoidal voltages for the PMSM. A general schematic of an inverter is shown at Fig. 4.

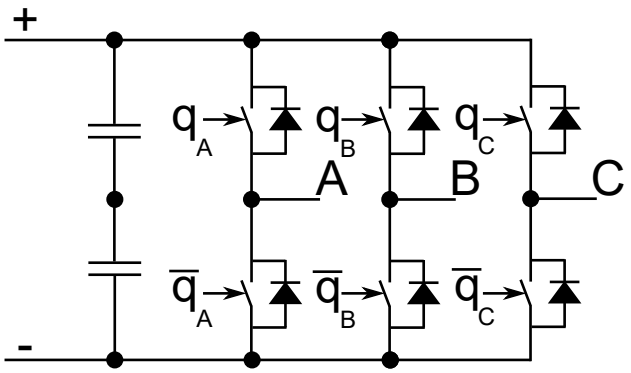

Fig. 4 A general inverter design for a three phase motor.

It is chosen to design a PCB with the inverter; besides this, some extra peripherals for the PCB are needed to be able to utilize a feedback control of the PMSM. The overall functions of the PCB are:

- Position feedback for PMSM by Hall or encoder sensors
- Gate drivers for the six external transistors
- Acceleration feedback for activation of PMSM with Gyroscope
- Current feedback for the three motor phases for the FOC control
- Plug-in system for DSP to control the different peripherals

For the design it is chosen to use a chip, which has the following functions: it can drive the gates of the transistors with an input from the DSP, it can provide current feedback from the three motor phases and it can supply the DSP with an integrated buck regulator. The chip is from Texas Instruments, and has the model name DRV8353RH [5].

For the half bridges, MOSFETs are used with the TO220 housing to make cooling easy. The half bridges are placed close to two relatively large (10000uF) capacitors, which are used as a DC-BUS to ensure a ripple free potential when fast switching is done. The rest of the components and configurations for the chip can be found in the project [6]. The complete PCB design is shown at Fig. 5.

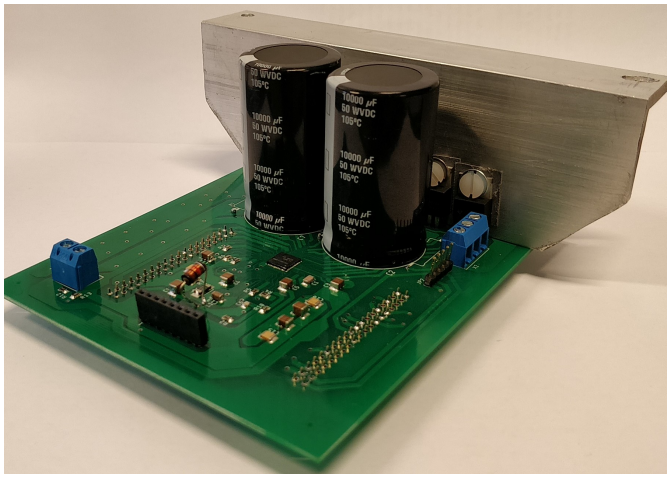

Fig. 5 A picture of the PCB where the DSP can be plugged in on the other side.

The STM32F446RE micro-processor is chosen as DSP to control the system. The processor has two advanced control timers which can produce 6 PWM signals to control the motor, 3 regular and 3 inverted. The advanced control timers can also read inputs from hall sensors. Other functionalities include ADC's and 180MHz clock speed providing good computational power.

4. Time Domain Model

To be able to simulate the dynamic and steady state response of the electro-mechanical system a mathematical time domain model has to be established. It begins with a model of the PMSM, which includes a transformation from the physical three phase circuit to a complex space vector orientation. After this, it translates the electrical torque from the PMSM into the mechanical system, where the PMSM is geared through the belt to the brush. The transformations are done with reference to the frame shown at Fig. 6.

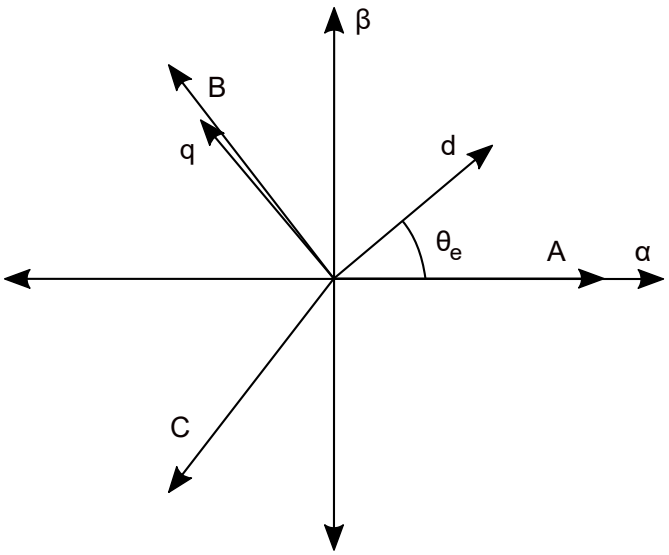

Fig. 6 The reference frame for the model of the PMSM.

The three axes A, B and C in figure 6 describe the orientation of the electrical phases for the PMSM, where each phase can be described with the equivalent electrical circuit shown in Fig. 7.

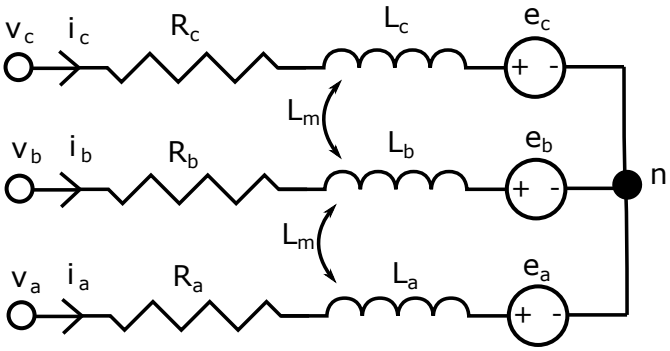

Fig. 7 An electrical schematic of the simplified circuit, with resistors, inductors and emf's all connected in the star point n.

To simplify the electric equivalent circuit some assumptions have been made: The windings resistance, inductance and mutual inductance are equal and considered constant, the small airgaps between the magnets are neglected, magnetic saturation, reluctance torque and temperature sensitivity are neglected and the back emf is considered sinusoidal. The voltage equations for each phase are expressed with (1) to (3).

$$v_{An} = R_A\, i_A + L_A \frac{di_A}{dt} + L_m\,(\frac{di_B}{dt} + \frac{di_C}{dt}) + \lambda \frac{d}{dt}\cos\theta_e \tag{1}$$

$$v_{Bn} = R_B\, i_B + L_B \frac{di_B}{dt} + L_m\,(\frac{di_A}{dt} + \frac{di_C}{dt}) + \lambda \frac{d}{dt}\cos\theta_e - \frac{2\,\pi}{3} \tag{2}$$

$$v_{Cn} = R_C\, i_C + L_C \frac{di_C}{dt} + L_m\,(\frac{di_A}{dt} + \frac{di_B}{dt}) + \lambda \frac{d}{dt}\cos\theta_e - \frac{4\,\pi}{3} \tag{3}$$

Where (R) is the resistance, (L) the inductance, (e) the back-emf, (λ) the flux linkage and (θ_e) the rotor position.

4.1 Clarke Transformation

The Clarke transformation transforms the reference frame (A, B, C) into the stator fixed reference frame (α,β). This is accomplished by using the matrix in equation (4).

$$\begin{bmatrix} k_\alpha \\ k_\beta \end{bmatrix} = \frac{2}{3} \begin{bmatrix} 1 & -\frac{1}{2} & -\frac{1}{2} \\ 0 & \frac{\sqrt{3}}{2} & -\frac{\sqrt{3}}{2} \end{bmatrix} \begin{bmatrix} k_A \\ k_B \\ k_C \end{bmatrix} \tag{4}$$

Here k is an arbitrary constant such as voltage or current. The Clark transformation can be utilized to reduce the voltage expressions (1) to (3) into a more simplified notation expressed with (5)

$$\vec{v_{\alpha\beta}} = R\,\vec{i_{\alpha\beta}} + (L_{ABC} - L_m)\,\frac{d\vec{i_{\alpha\beta}}}{dt} + \lambda\, j\,\omega_e\, e^{j\theta_e} \tag{5}$$

Here L_{ABC} and R defines the individual phase resistance and inductance. In the next section this expression is transformed into the rotating reference frame (d,q).

4.2 Park Transform

The Park transformation transform a rotating space vector in the (α,β) reference frame into a space vector in the rotating (d,q) frame. The advantage of this is that any position dependencies in the equations are cancelled out. The (d,q) frame is rotating with the electrical velocity (ω_e). To perform the Park transformation, the rotation matrix equation (6) is used.

$$\begin{bmatrix} k_d \\ k_q \end{bmatrix} = \begin{bmatrix} \cos\theta_e & \sin\theta_e \\ -\cos\theta_e & \sin\theta_e \end{bmatrix} \begin{bmatrix} k_\alpha \\ k_\beta \end{bmatrix} \tag{6}$$

By applying the transformation to the equation 5 the simple expression (7) emerges.

$$\begin{aligned} \vec{v_{dq}} &= R\,\vec{i_{dq}} + L_{dq}(\frac{d\vec{i_{dq}}}{dt} + j\,\omega_e\,\vec{i_{dq}}) + j\,\omega_e\,\lambda \\ &= R\,\vec{i_{dq}} + L_{dq}\frac{d\vec{i_{dq}}}{dt} + j\,\omega_e\,(L_{dq}\,\vec{i_{dq}} + \lambda) \end{aligned} \tag{7}$$

This can be expanded to the individual axes of d and q with equation (7) which defines two simple electrical circuits with DC signals for the motors dynamic behavior.

$$u_d = \Re u_{dq} = R\, i_d + L_d \frac{di_d}{dt} - \omega_e\, L\, i_q \tag{8}$$
$$u_q = \Im u_{dq} = R\, i_q + L_q \frac{di_q}{dt} + \omega_e\, (L\, i_d + \lambda)$$

From these electrical circuits a corresponding electromagnetic torque τ_e can be described for the PMSM with equation (9).

$$\tau_e = \frac{3\,\lambda\, z_p\, i_q}{4} \tag{9}$$

This torque is transferred into the mechanical system which will be described in next section.

4.3 Mechanical System

The mechanical system consists of the PMSM, the gearing and the brush. The system is described with reference to the motor side of the gearing, so if a load torque is applied to the brush it is transferred through the gearing to the motor. The resulting moment acting on the mechanical system is modelled as the electrical torque subtracted from friction losses and a load torque with equation (10).

$$\frac{d\omega_m}{dt}\, J_{eq} = \tau_e - B\, \omega_m + \mathrm{sgn}(\omega_m)\, \tau_{df} - \frac{1}{N}\, \tau_{load} \tag{10}$$

Here (B) is the viscous damping coefficient, J_{eq} is the equivalent inertia of the system, (τ_{df}) is the static friction of the system, (τ_{load}) is a load torque and (ω_m) the mechanical velocity.

4.4 Nonlinear and Linear systems

The model of the electromechanical system can be described with the three differential equations (11) to (13).

$$\frac{d\omega_m}{dt} = \frac{1}{J_{eq}} \left(\tau_e - B\, \omega_m + \mathrm{sgn}(\omega_m)\, \tau_{df}\right) \tag{11}$$
$$\frac{di_d}{dt} = \frac{1}{L_d}\, v_d - \frac{R}{L_d}\, i_d + \frac{z_p}{2}\, \omega_m\, i_q \tag{12}$$
$$\frac{di_q}{dt} = \frac{1}{L_q}\, v_q - \frac{R}{L_q}\, i_q - \frac{z_p}{2}\, \omega_m\, i_d - \frac{z_p}{2}\, \omega_m\, \frac{\lambda}{L_q} \tag{13}$$

By neglecting the nonlinear terms of the equations, a linear model can be obtained which then can be transformed into transfer function with the use of the Laplace transform. The linear representation is expressed with (14) to (16).

$$\frac{\omega_m(s)}{i_q(s)} = \frac{\frac{3\,\lambda\, z_p}{4}}{J\, s + B} \tag{14}$$
$$\frac{i_d(s)}{v_d(s)} = \frac{1}{L_d\, s + R} \tag{15}$$
$$\frac{i_q(s)}{v_q(s)} = \frac{1}{L_q\, s + R} - \frac{\omega_m(s)}{v_q(s)}\, \frac{z_p\, \lambda}{2\, L_q} \tag{16}$$

4.5 Parameter Identification

The unknown parameters needed to be identified for the model are: Phase resistance (R), synchronous inductance (L_d, L_q), flux linkage amplitude (λ), moment of inertia (J) and friction coefficients (B, τ_{df}).

4.5.1 Phase resistance

The phase resistance is determined with a DC source, where the line to line resistance is assumed to be linear. A set of different voltages and currents is collected and shown at Fig. 8. A proportional regression is then utilized to indicate the slope, where the phase resistance is equal to half of the slope which gives 0.22Ω.

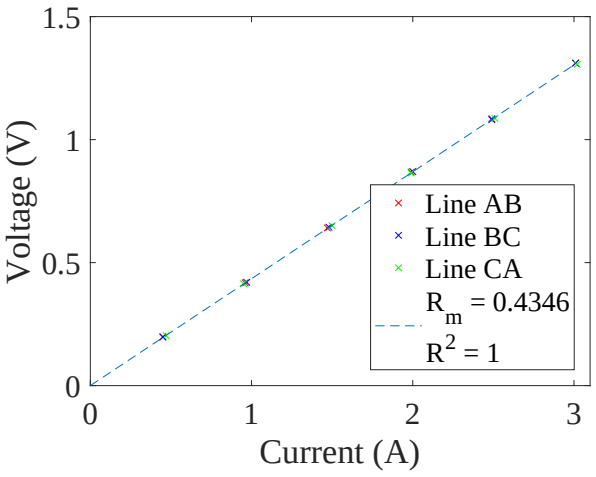

Fig. 8 Collected resistans measurements with a proportional regression.

4.5.2 Synchronous inductance

The inductances are measured with an AC steady-state impedance method with reference to [7] that consist in aligning the PMSM to the q or d-axis and then lock the rotor mechanically. Hereafter, an AC voltage is applied, where two of the phases are connected to the negative potential and one phase to the positive. The inductance will consist of 1.5 times the phase inductance. By knowing R from the previous

experiment and calculating the impedance (Z) with the rms values of voltage and current the reactance (X) can be calculated with equation (17).

$$X = \sqrt{Z^2 - R^2} = \sqrt{\frac{V^2}{I^2} - R^2} \tag{17}$$

Knowing X and the frequency of the AC signal f the inductance is calculated with equation (18).

$$L = \frac{2}{3}\frac{X}{2\pi f} \tag{18}$$

The collected measurements for the voltage, current and inductance for the q-axis are shown at Fig. 9 and Fig.10.

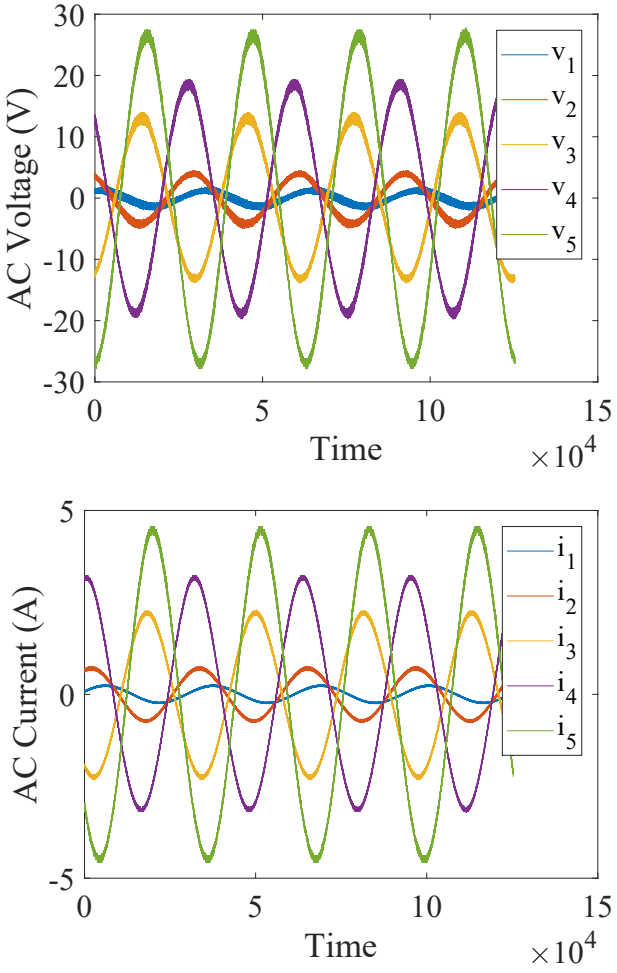

Fig. 9 Collected measurements for different AC signals with 100Hz for the q-axis.

From Fig. 10 it is seen that the tendencies for the inductance are constant. The resulting inductances for both the d and q-axis are listed in Tab.I.

Frequency	L_d	L_q	Unit
100Hz	6.23	6.63	mH
500Hz	4.05	4.77	mH

Tab. I The mean inductance for two frequencies and axes.

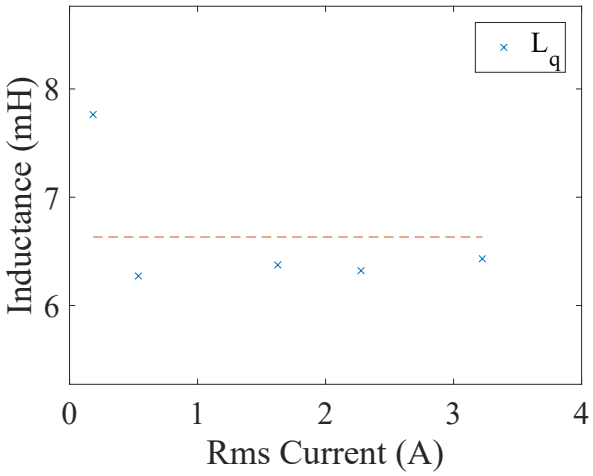

Fig. 10 Collected measurements for synchronous inductance in the q-axis with 100Hz

4.5.3 Flux Linkage Amplitude

The flux linkage amplitude λ can be theoretically calculated by the peak amplitude (e_{peak}) divided by the electrical velocity (ω_e) as in equation (19).

$$\lambda = \frac{e_{peak}}{\omega_e} \tag{19}$$

It can also be measured by a test where the rotor is rotated with a drill machine, at a constant velocity, where the PMSM is not electrical connected. Thereby the induced voltage from the flux linkage can be measured with an oscilloscope, where the induced phase back emf will be shown if the oscilloscope is connected to one of the phases and the neutral point. The experimental value found is equal to λ=0.0213Wb.

4.5.4 Moment of inertia

The equivalent moment of inertia is calculated by the conservation of kinetic energy, where the inertia of the structural components is estimated with the CAD drawings. The equivalent inertia for the system is J_{eq}= 0.14kgm^2.

4.5.5 Friction coefficients

A run out test is performed for determining the friction coefficients. The test is performed by driving the Cowbrush with an initial constant angular velocity and then suddenly turning off the motor, causing the system to decelerate due to the friction in the system. By measuring the decelerating velocity over time, it is possible to fit a friction model. The deceleration is collected for different initial velocities, and compared to see if the parameters are constant or how much they

vary. The values obtained are $B = 0.0273 NmRad/s$ and $\tau_{df} = 0.03 Nm$.

An example of two velocity profiles and the fitted curves is shown at Fig. 11.

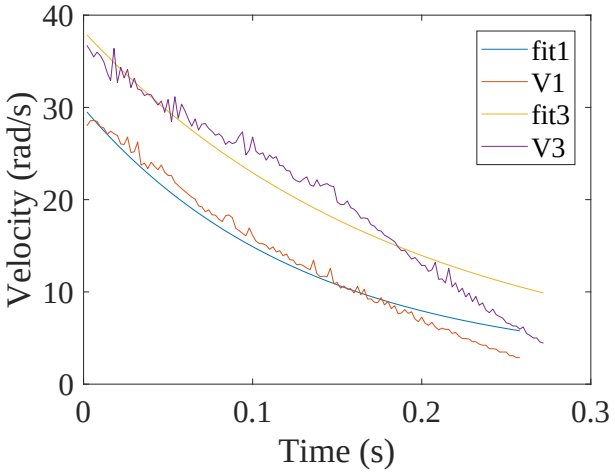

Fig. 11 Collected velocity measurements for two test with the corresponding fits.

5. Control Stratey

The control strategy for the system is a Field Orientated Control (FOC), where a torque control of the motor will be designed. The torque control is chosen to utilize a smooth operation of the brush even though the loads from the cow are expected to be very irregular.

A block diagram describing the FOC strategy for the system is shown at Fig. 12.

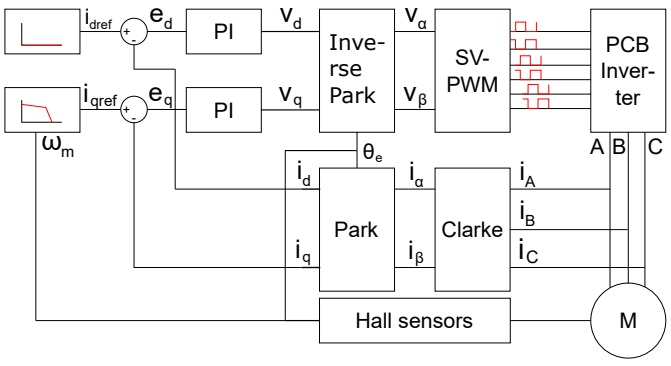

Fig. 12 Field Oriented Control structure

Two PI controllers are chosen for the system, which will provide a constant voltage at steady state and thereby a constant velocity of the brush.

The torque reference for the PMSM is chosen to be like the original single phase induction machine, where the torque speed characteristic is approximated with two linear lines. This is shown at Fig.13.

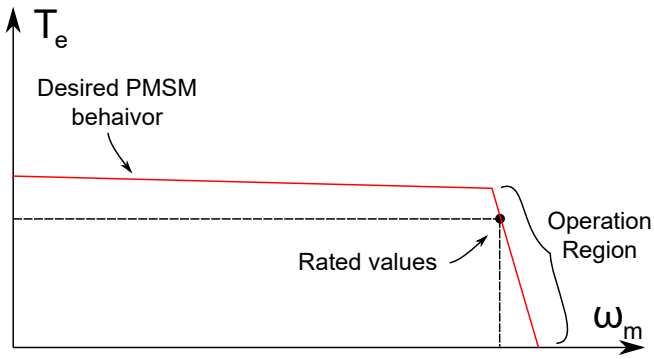

Fig. 13 An illustration of the desired torque speed characteristic for the PMSM.

The operating region for the motor is chosen based on the wishes from GEA, where a brush operating velocity of $35 Rpm$ was desired. Therefore it seems sensible to control the motor with an operating region of 30-40Rpm for the Brush which geared gives a motor velocity of 130-180Rpm. Besides this the motor have to be able to deal with a load of 25Nm in the region, which is a load postulated from the earlier concept study [3]. This has lead to the determination of a maximum operation torque of 26.4Nm at $30 Rpm$, which for the motor is equal to 5.88Nm at $130 Rpm$.

By converting the desired torque speed curve into a current speed curve instead, a reference is established for the current controller in the q-axis. This reference is shown at Fig. 14.

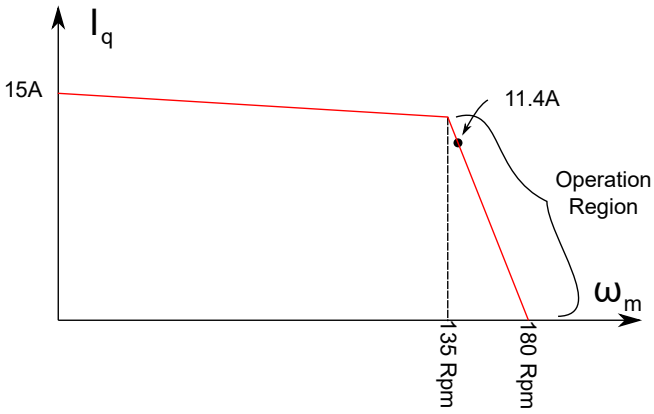

Fig. 14 An illustration of the desired current reference of the q-axis controller depending on the motor speed.

The requirements for the PI controllers are categorized with stability and loads. For the stability it is required that the controller is stable but also relatively stable with a phase margin beyond 45° and a gain margin of

minimum 8 dB. For the load case, it is required that the controller can handle step loads of maximum 26.4Nm, with a maximum percentage error of 5%.

5.1 PI design

The controller is designed for the linear transfer functions derived in section 4. Here it is chosen to use the same controller parameters for both the d and q-system. The controllers are tested with an implemented linear system in SIMULINK which is shown at Fig. 15.

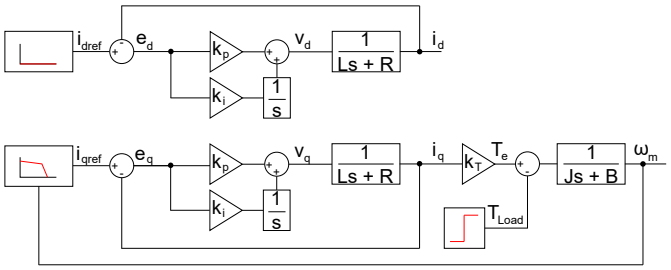

Fig. 15 Block diagram of the linear system.

The general PI controller is expressed with the transfer function in equation (20) where k_p is the proportional gain and k_i is the integral gain.

$$G_c(s) = k_p + \frac{K_i}{s} \tag{20}$$

The optimal design will be to place the zero upon the pole from the plant and thereby achieve a pure integrator response. But this can be difficult to obtain because it might need a large energy source.

Therefore it is chosen to investigate the largest deceleration of the system if a cow applies 26.4Nm modelled as a step. This would give a deceleration of $42s^{-2}$. This indicates the slope of the change in torque, which needs to be handled by the controller to ensure a track of the reference. Here the initial gains were chosen as 80% of the value for the proportional gain and 20% for the integral gain which were normalized with respect to the DC gain of the system.

After tuning with the linear model a final set of values where obtained for the controllers, k_p = 8.32 and k_i= 3.75, which simulated results are shown at Fig. 16.

The k_i could be increased more, to achieve a smaller error faster, but the controller is capable of tracking the reference within the percentage requirements already so it is left as it is.

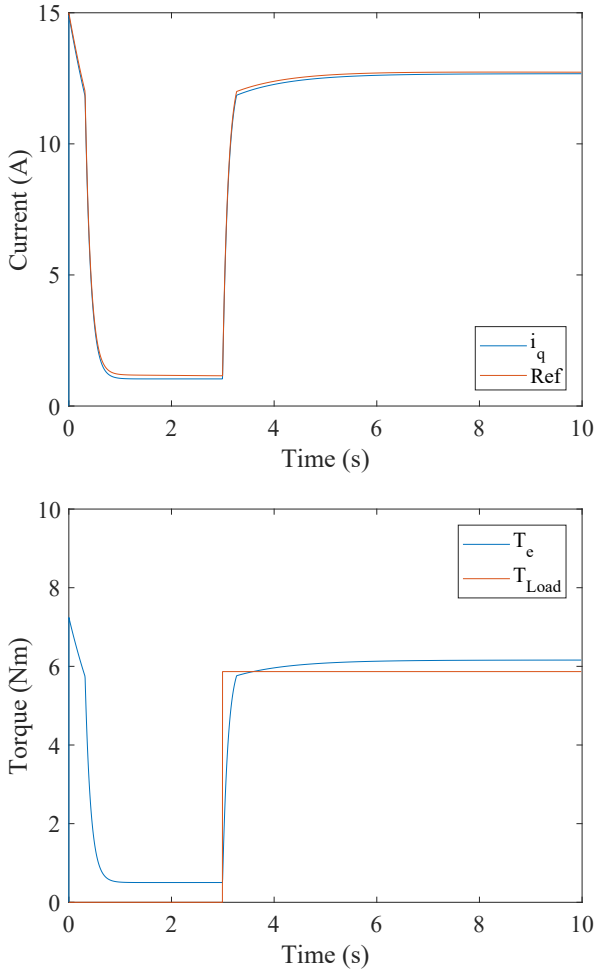

Fig. 16 Simulation of final controller parameters; Top: Plot of the i_q current and the reference. Bottom: the developed electromechanical torque and applied load step.

5.2 Discrete System

The continuous system needs to be transformed into a discrete system, because the DSP cannot handle continuous time signals. The discrete system is developed with the method of emulation, where the continuous controller and plant is mapped into the z-domain. Here the important parameter is the sampling time (T_s), because this time can make a s-stable controller z-unstable. The sampling time for the system will be chosen with a rule of thumb, that says that the sampling frequency should be ten times faster than the bandwidth. In this case it will require a sampling frequency of 2kHz. The discrete open loop transfer function for the system is expressed with equation (21).

$$G(z) = \left(k_p + \frac{T\,k_i\,(z+1)}{2\,z-2}\right) k_{DC}\,\frac{1-e^{-T}}{z-e^{\frac{-R}{L}T}} \tag{21}$$

5.2.1 Difference equations

The z-domain controller needs to be described as a difference equation to be able to implement it on the DSP. The controller pulse transfer function for the controller is expressed with equation (22).

$$\frac{M(z)}{E(z)} = k_p\, 2\, z - 2\, k_p + T\, k_i\, z + T\, k_i \qquad (22)$$

By rearranging the expression and division with z it can be transformed into a difference equation like equation (23).

$$m(kT) = k_p\, e(kT) - k_p\, e(kT-1) + \frac{1}{2}\, k_i\, e(kT) + \frac{1}{2}\, T\, k_i\, e(kT-1) + m(kT-1) \qquad (23)$$

The expression is used for both the d and q axis controller in the DSP, where T_s = 0.0005s. Besides this a saturation limit is also used in the DSP to ensure that the integrator part does not windup.

6. Conclusion

The conclusion is based on the workload for the project which is referred to with [6].

The original E-brush power transmission was found to be inefficient due to the single phase induction motor which was coupled with a worm gear. Therefore a new concept design had to be developed.

A simple functional analysis was performed, which was based on a belt/chain driven drive train. Here, a concept design with a polyvee belt drive was developed, with a tension mechanism. The chosen belt gearing was designed to exploit the housing in the best possible way, which lead to a gearing ratio of 4.5. The performance of the polyvee belt has an efficiency of almost 100%. Finally, the concept was constructed such that the PMSM and the belt drive could be mounted on a support plate which is universal for other Cowbrush units as desired.

An already existing converter was utilized to convert the grid line voltage into a DC supply voltage for the electrical circuit.

It can be concluded that a Printed Circuit Board (PCB) was developed, which theoretically can invert a DC source of 10 to 100V with a variable frequency up to 20kHz. It can also be concluded that the PCB can obtain feedback signals from a PMSM, for both current measurements of each phase and position measurements from a hall/ encoder sensor. The PCB was designed to fit together with a DSP from STM, which could control the peripherals of the PCB, consisting of the gate drivers for the external MOSFETs, the Gyroscope for the activation, the current and position feedback signals and the FOC control strategy for the PMSM.

It can be concluded that a nonlinear model of the Cowbrush unit was established, which included an electrical model of the PMSM and a mechanical model of the drive train.

It can be concluded that the electrical model transform the three phase circuit into a rotor fixed circuit of two components instead. This transformation is done with a Clarke and a Park transformation.

It can be concluded that the nonlinear model parameters are obtained through laboratory test, to be able to simulate the dynamic and steady state responses of the system. With the experimental tests the parameters where found which is listed in Tab. II.

Parameters	Values
R	0.22Ω
L	4 - 6.3mH
λ	0.0216Wb
J	0.14 kg m^2
B	0.0273 Nm Rad/s
τ_{df}	0.03Nm

Tab. II Model parameters obtained through experimental test.

The nonlinear model was transferred into linear transfer functions by neglecting the nonlinear couplings. The transfer functions where studied, where it was found that they both where stable. Besides this the sensitivity of the electrical system was investigated, which showed that the variation in the resistance could be neglected and that the variation in the inductance could change the system significantly.

It can be concluded that a FOC control strategy was developed for the model, where two linear PI contollers are designed. The resulting parameters for the controllers was a proportional gain of 8.32 and a integral gain of 3.75. These parameters was tested in the nonlinear and linear models, where it can be concluded that they meet the requirements.

Acknowledgement

The authors of this work gratefully acknowledge

Grundfos for sponsoring the 7th MechMan symposium.

References

[1] Dyrlæger og ko, Lov om hold af malkekvæg - hvilke nye regler træder i kraft pr. 1. juli 2016? Dyrlæger og ko, 2019. Visited 2019-11-04.

[2] Eric Metzger, Making the case for cow brushes. Progressive Dairyman, 2019. Visited 2019-11-04.

[3] F. C. A. L. A. T. S. Borup, M. Brandt, "Concept study of pm synchronous motor drive system in cow brush application," Mechman, April 2019.

[4] P. R. N. Childs, Mechanical design engineering handbook. Elsevier Science and Technology, 2013.

[5] TEXAS INSTRUMENTS, DRV835x 100-V Three-Phase Smart Gate Driver, 2019.

[6] K. L. E. Olesen, R. Starup-Hansen, "Control and implementation of a permanent magnet synchronous motor in cowbrush unit," Mechman, May 2019.

[7] W. L. Soong, "Inductance measurements for synchronous machines," Power Engineering Briefing Note Series, April 2019.